

*Supplementary Materials*

**Optetrode: a multichannel readout for optogenetic control  
in freely moving mice**

Polina Anikeeva<sup>1\*</sup>, Aaron Andalman<sup>1\*</sup>, Ilana Witten<sup>1</sup>, Melissa Warden<sup>1</sup>, Inbal Goshen<sup>1</sup>, Logan  
Grosenick<sup>1</sup>, Lisa Gunaydin<sup>1</sup>, Loren M. Frank<sup>4</sup>, and Karl Deisseroth<sup>1,2,3,5</sup>

<sup>1</sup> Department of Bioengineering

<sup>2</sup> Department of Psychiatry and Behavioral Sciences

<sup>3</sup> Howard Hughes Medical Institute

Stanford University, Stanford, CA, U.S.A.

<sup>4</sup> Department of Physiology, University of California, San Francisco, CA, U.S.A.

\* These authors contributed equally

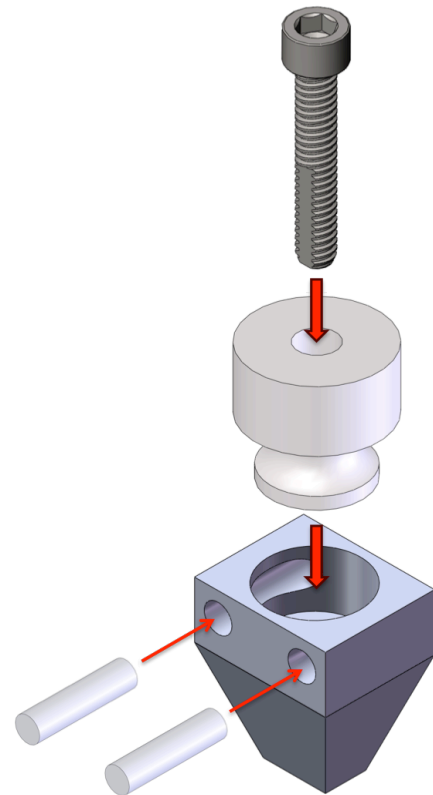
## Supplementary Note: Optetrode step-by-step fabrication instructions.

### I. Tetropdes

- 1) Use epoxy to glue ~16 mm long plastic tubing to the screw hole next to the ground pin-hole of the EIB-16. Plastic tubing should rise ~0.3-0.5 mm above the EIB-16 in order to prevent glue from getting inside. Plastic tubing should protrude ~14 mm under the EIB-16. Let the epoxy dry for at least 15 min.
- 2) Cut ~5 cm long ground wire. Burn or strip plastic coating off the wire ~1 cm at each end. Use a gold pin to attach the ground wire to the EIB. It may be necessary to widen the pin-hole beforehand by pushing in a pin.
- 3) Make 4 tetropdes following standard protocols reported in literature (e.g. Ref. 18)
- 4) Affix the tetropdes to the EIB-16. Feed the 16 individual ends of the wires into the 16 pin-holes of the EIB-16 following the bottom up direction. Fix the wires to the EIB-16 with gold pins. The EIB-16 should now have a guiding tube and 4 tetropdes hanging underneath.
- 5) Use soldering iron to melt the gold pins into the pin-holes. Press hot iron to each pin for ~10-15 seconds. Also do this for the ground wire.
- 6) Feed the tetropdes through the guiding tube.

### II. Drive

- 1) Screw the vented screw into the thumbnut half way, so that the bottom half is protruding from the thumbnut by 2-3 mm.
- 2) Insert the screw-thumbnut assembly into the plastic housing. It will only fit in the designed orientation in which flattened facets of the vented screw align with the flat sides of the tunnel of the plastic housing.
- 3) Fix the thumbnut to the plastic housing with the interference dowel pins. From this point turn the thumbscrew counterclockwise to lower the screw through the housing. Lower the screw to near the end of its range of motion.



### III. Assembly

- 1) Use a tall holder (e.g. optics post) to suspend the EIB-16 with tetrodes above the mechanical drive affixed to a shorter holder.
- 2) Lower the EIB-16 towards the drive, so that tetrodes go into the vented screw first, followed by the protective tubing until the EIB-16 is flush with the cap of the vented screw.
- 3) Use a fiber-ferrule cut to the length appropriate for the experiment. The fiber length should be sufficient to protrude from the vented screw and reach the area of interest within the travelling distance of the vented screw.
- 4) Lower the fiber-ferrule into the plastic tubing.
- 5) Use Superglue or equivalent to attach the tetrodes to the fiber and wipe excess glue. At this point, the tetrodes should still be significantly longer than the fiber-ferrule; hence coating them in glue does not pose a problem. Use a small amount of glue to fix the fiber-ferrule to the guiding tube and EIB. It is important to ensure that some glue penetrates inside the vented screw; this will insure a good seal. Wait for glue to dry completely (~15 min).
- 6) Use 2-part epoxy to attach the fiber-ferrule to the EIB-16.

### IV. Finishing. This part should be done one night before or the morning of surgery.

- 1) Perform a final cut of the tetrodes <1 mm below the fiber. Measure impedance. It should be 4-8 M $\Omega$ .
- 2) Electrochemically deposit colloidal gold onto tetrode tips until impedance drops to <400 k $\Omega$  (e.g. Ref. 18).
- 3) Use epoxy to cover the EIB-16 and all the exposed wires. This will protect the device from animal-related damage, while insuring structural integrity.

## Supplementary Figures

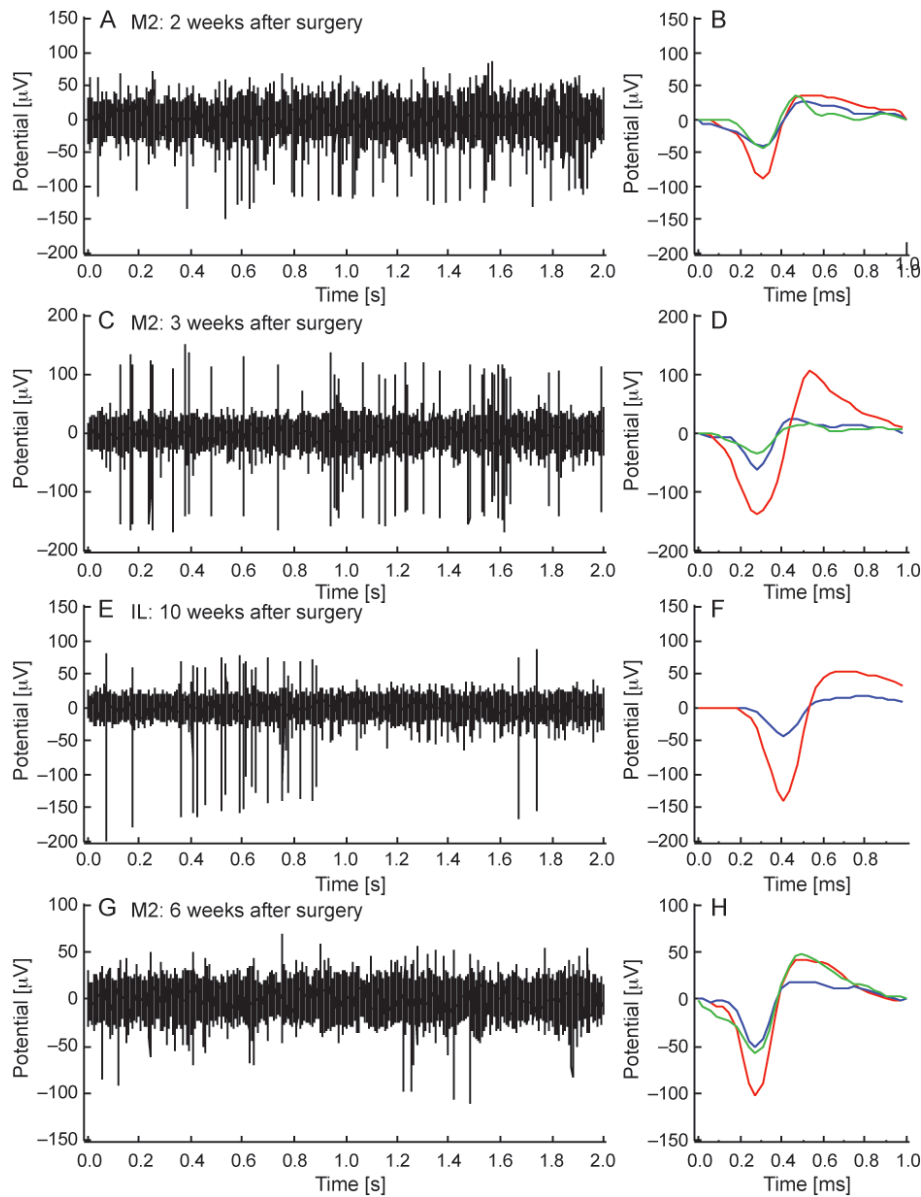


**Figure S1. Recording stability.** (a) Sample recording from M2 two weeks after the virus injection and optetrode implantation surgery. (b) Corresponding shapes of the action potentials recorded in (a) from three clusters. (c) Sample recording from M2 three weeks after the virus injection and optetrode implantation surgery (one week after the recording in (a)). Device had not been moved since surgery. (d) Corresponding shapes of the action potentials recorded in (c) from three clusters. (e) Sample recording from IL ten weeks after the virus injection and optetrode implantation surgery (seven weeks after the recording in

(c)). Device has been continuously propagated from the M2 down to IL (total distance traveled 1.6 mm). (f) Corresponding shapes of the action potentials recorded in (e) from two clusters. (g) Sample recording from M2 of a different animal six weeks after the virus injection and optetrode implantation surgery. Device had not been moved since surgery. (h) Corresponding shapes of the action potentials recorded in (g) from three clusters.

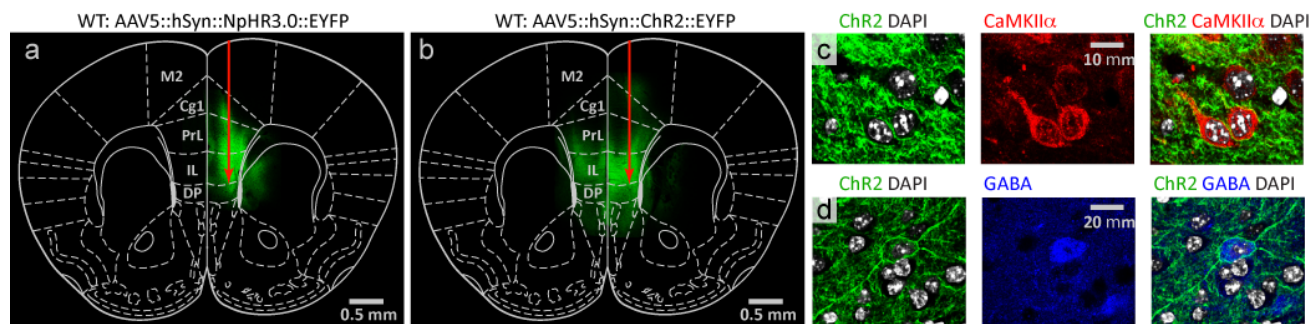


**Figure S2. Confocal images of the medial prefrontal cortex of wild type mice expressing ChR2::EYFP or NpHR3.0::EYFP under the hSyn promoter.** (a), (b) Expression profiles of eNpHR3.0-EYFP and ChR2-EYFP. (c), (d) Micrographs of CaMKII $\alpha$  and GABA neurons expressing ChR2-EYFP.

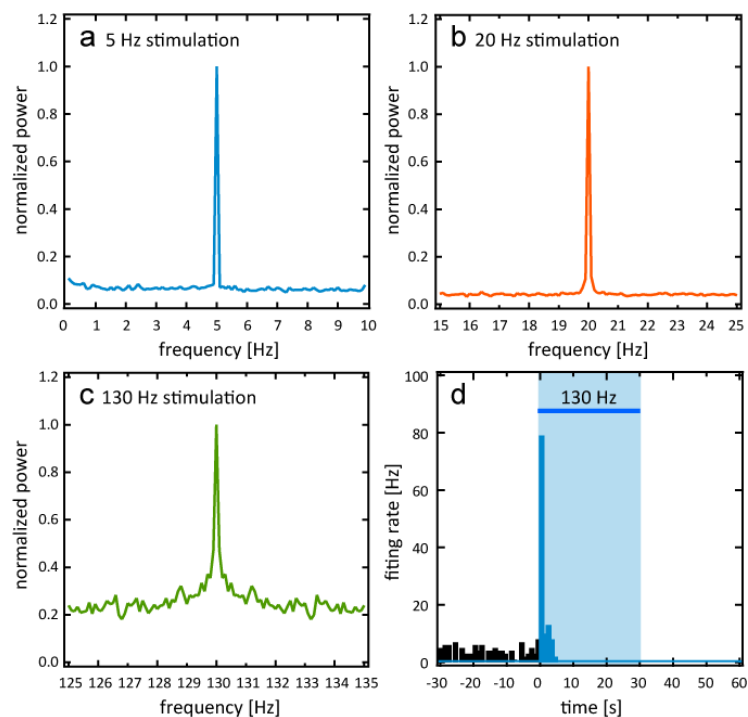


**Figure S3. Power spectra of the light-evoked neural activity in wild type mice expressing ChR2 under hSyn promoter.** (a), (b), (c) Fourier power spectra of multi-unit responses to optical stimulation at 5 Hz (a), 20 Hz (b) and 130 Hz (c) (473 nm, 5 ms pulse width). Sharp peaks at 5 Hz in (a) and 20 Hz in (b) signify coherence of the multi-unit response with the stimulation pulses. The presence of the high background in (c) corresponds to loss of coherence of the multi-unit response with laser pulses at 130 Hz stimulation. (d) Example trace of the long-term inhibition of multi-unit activity by 130 Hz stimulation. Light is applied between 0 and 30 seconds.

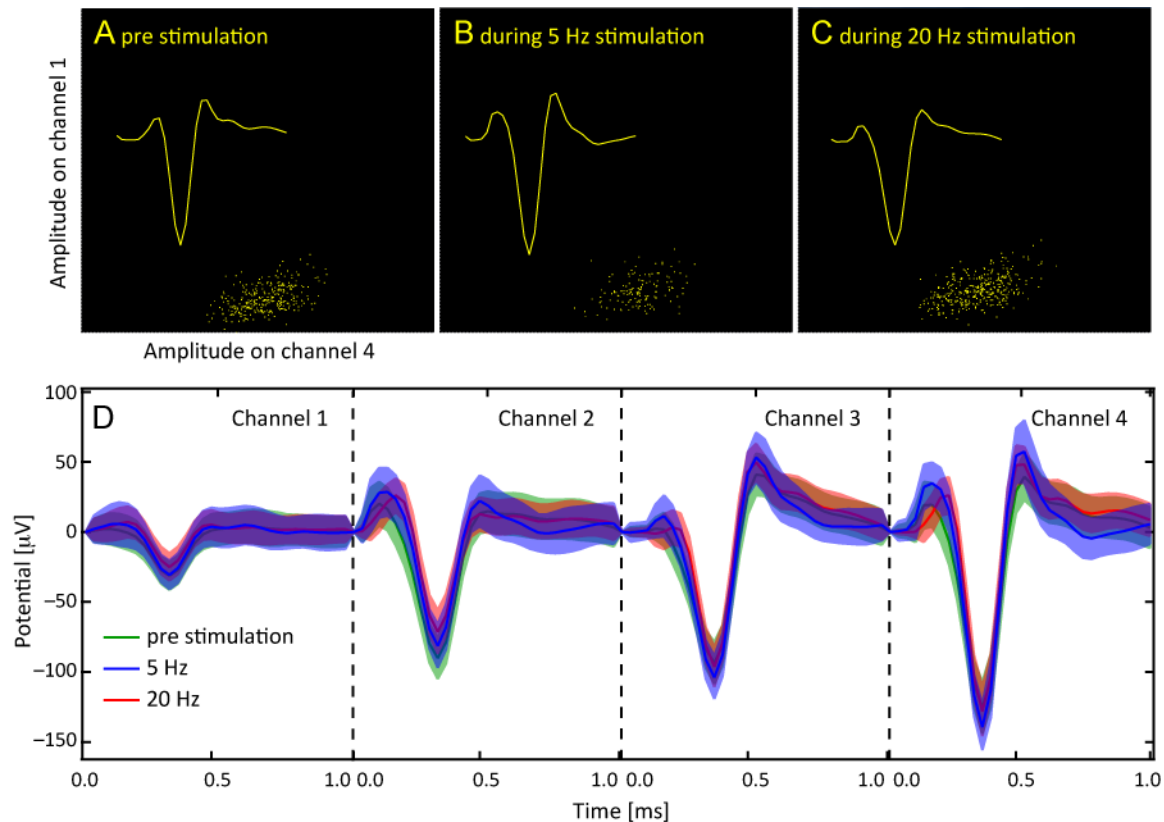


**Figure S4. Examples of action potential shapes prior to and during optical stimulation in wild type mice expressing ChR2 under hSyn promoter.** (a), (b), (c): Action potential amplitudes on channels 1 and 4 of a tetrode bundle, plotted against each other. Cluster represents an individual neuron (this unit is also shown in Fig. 2g-i). (a) The amplitude cluster and the action potential shape prior to optical stimulation. (b) The amplitude cluster and the action potential shape during 5 Hz optical stimulation (wavelength  $\lambda=473$  nm, 5 ms pulse width). (c) The amplitude cluster and the action potential shape during 20 Hz optical stimulation (wavelength  $\lambda=473$  nm, 5 ms pulse width). (d) The average action potential shapes on the 4 channels of a tetrode bundle demonstrate recording of the same unit prior and during 5 Hz, and 20 Hz stimulation. Shaded area represents standard deviation.

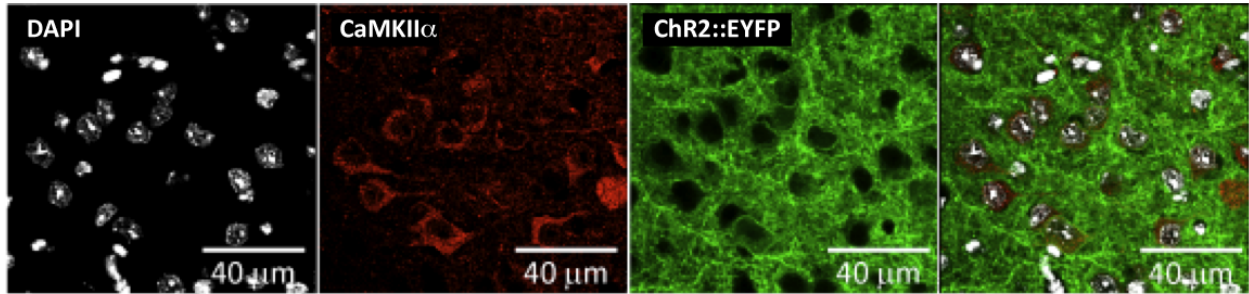


**Figure S5. Confocal images of the medial prefrontal cortex of wild type mice expressing ChR2::EYFP under the CaMKII $\alpha$  promoter.**

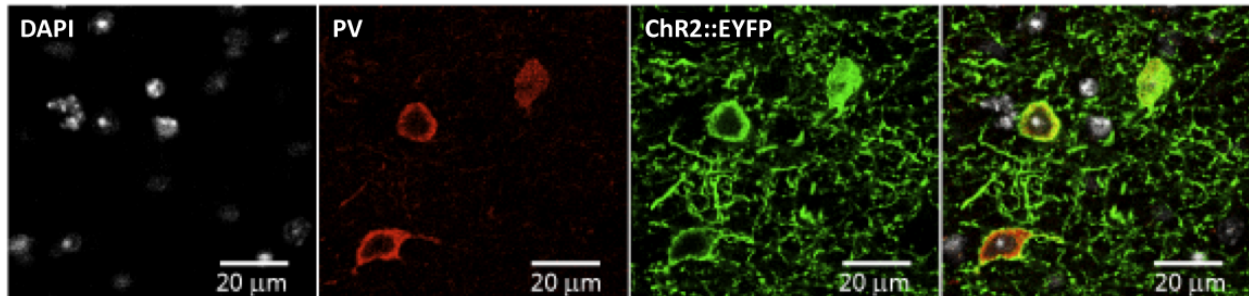


**Figure S6. Confocal images of the medial prefrontal cortex of PV::Cre mice expressing ChR2::EYFP under DIO control.**

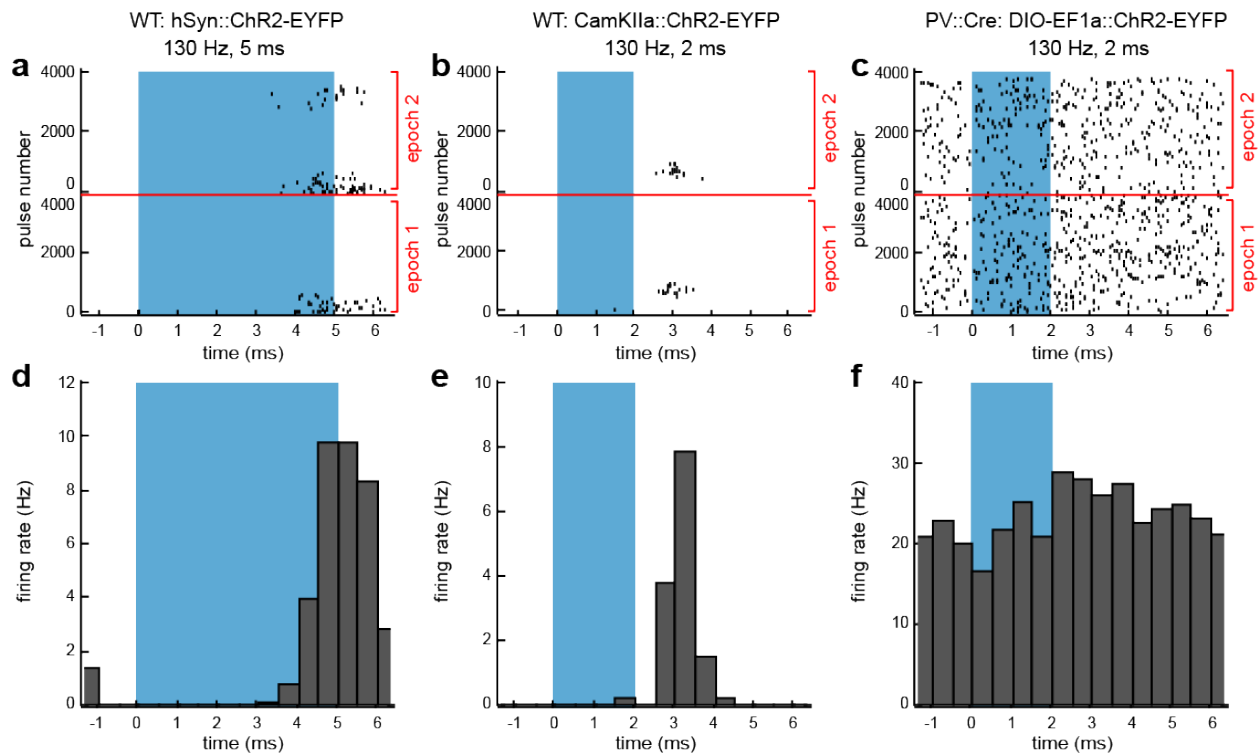


**Figure S7. Raster plots of neural activity during 130 Hz optical stimulation in wild type mice expressing ChR2 under the hSyn and CaMKII $\alpha$  promoters and in PV::Cre mice expressing ChR2 in PV cells.** (a), (b), (c) Spike rasters for single units recorded during two 30 second epochs of stimulation in the mPFC in: (a) a wild type mouse expressing ChR2 under the hSyn promoter; (b) a wild type mouse expressing ChR2 under the CaMKII $\alpha$  promoter; and (c) a PV::Cre mouse expressing ChR2 in PV+ neurons under a DIO construct. Spikes (black dots) are shown in a 7.7 ms (one full period at 130Hz) observation window around each light pulse. (a) This neuron (shown in Fig 2i-k) spiked with short latency following each light pulse (blue background) at the beginning of each 30-second stimulation epoch but subsequently was largely silenced. During the second stimulation epoch the neuron produced a short burst of activity late in the epoch. The periods of suppressed activity could be due to depolarization block or to network effects induced by 130Hz stimulation. (b) This neuron (shown in Fig 3d-f) did not respond to light immediately following the start of each 30-second stimulation epoch, skipping >100 pulses, but then began spiking with short latency following each 2-ms light pulse, and then became silenced. (c) The firing rate of this neuron (shown in Fig 3i-k) showed higher baseline activity. (d), (e), (f) Light-pulse triggered spike histograms for the neurons shown in (a), (b), (c) respectively.

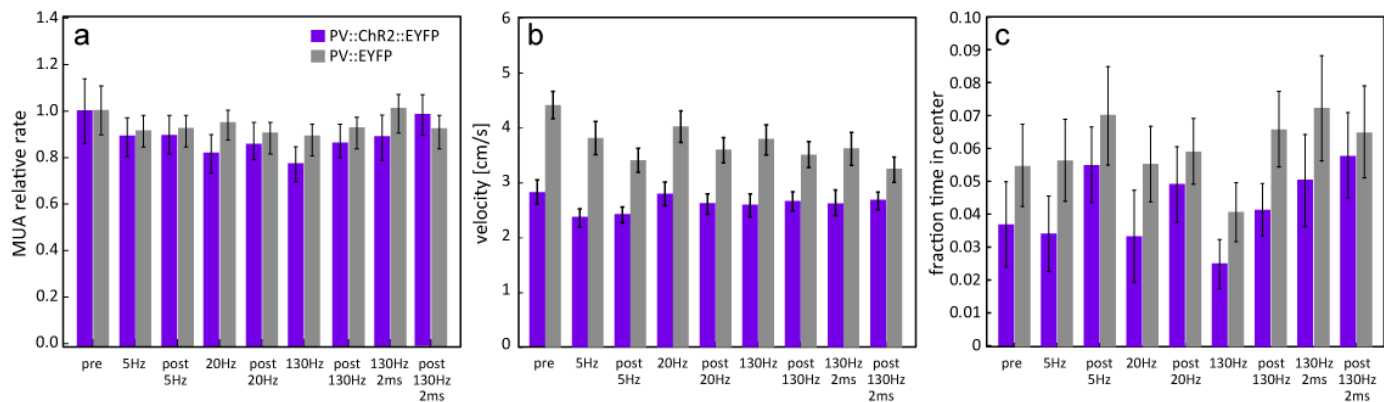


**Figure S8. Multi-unit activity rate, velocity and fraction time in center for PV::Cre positive and PV::Cre negative control mice prior, during and post light stimulation.**

Mice were subjected to the 22-minute open field exploration task and exposed to 30-second light stimulation epochs every two minutes. The stimulation parameters used were 5 Hz, 20Hz and 130 Hz with 5ms pulse width, or 130Hz with 2ms pulse width. Each stimulation type was used exactly twice but the order was randomized. (a) Normalized average multi-unit firing rate, (b) velocity and (c) percent time spent in the center of the open field for PV::Cre type mice expressing ChR2 in mPFC (purple; 28 OFTs in 2 mice) compared to EYFP expressing PV::Cre controls during and following each stimulation epoch (gray; 26 OFTs in 3 mice). With respect to velocity, note that the two cohorts displayed modestly different baseline velocity ( $p < 0.01$ , two-way ANOVA), but this was likely an idiosyncrasy of the two cohorts at baseline; there was neither a significant effect of light stimulation nor a significant light stimulation by cohort interaction ( $p = 0.18$  and  $p = 0.60$  respectively).

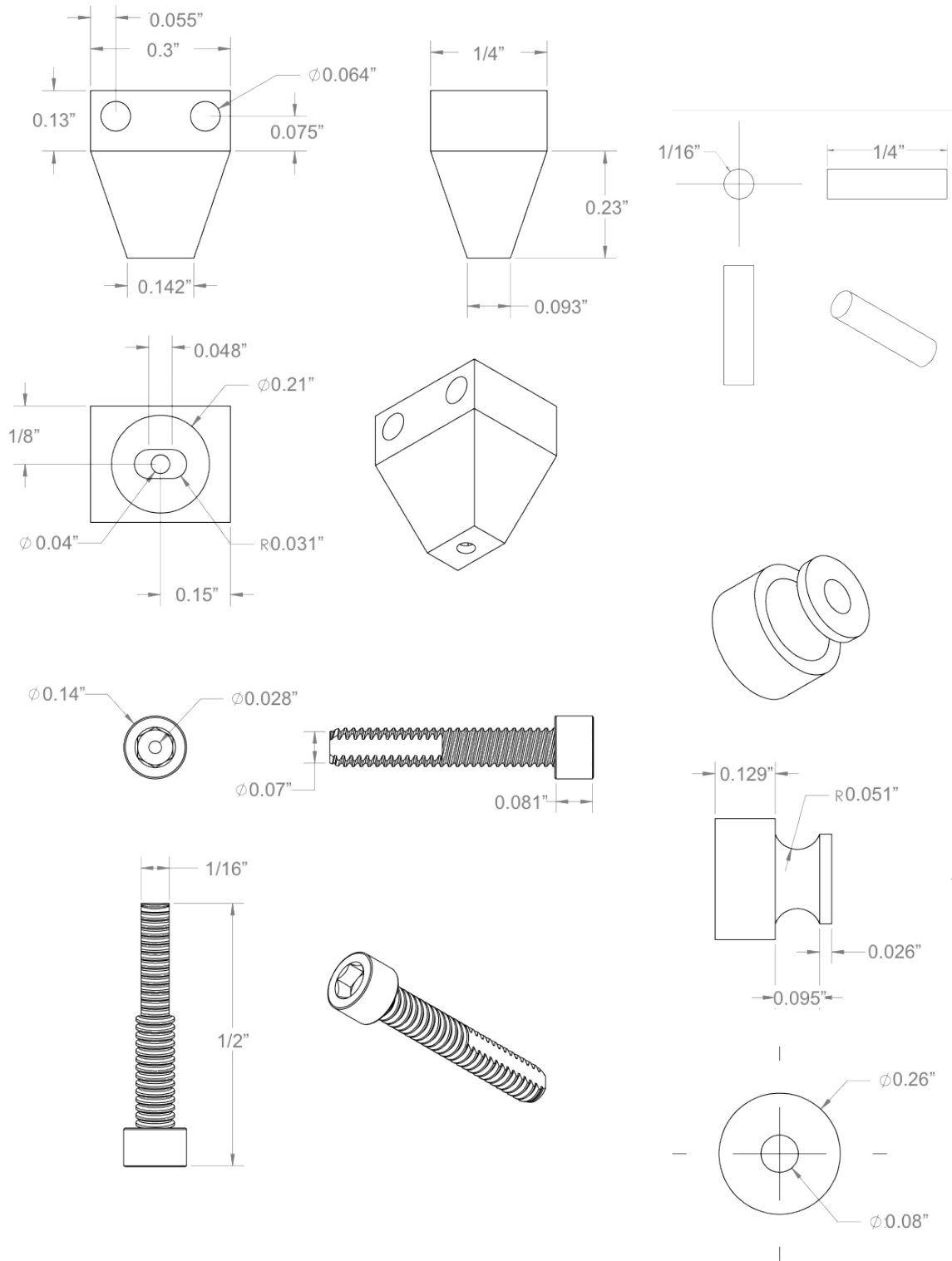


**Figure S9.** Optetrode mechanical drive design drawings (see step-by-step fabrication diagrams above).